NASA TECHNICAL NOTE

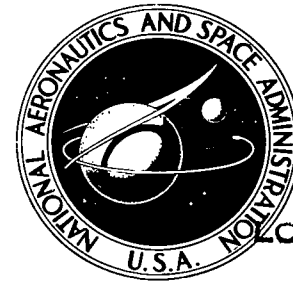

NORMAL IMPINGEMENT LOADS DUE TO SMALL AIR JETS ISSUING FROM A BASE PLATE AND REFLECTING OFF A PLATFORM FOR VARIOUS JET MACH NUMBERS, SEPARATION DISTANCES, AND AMBIENT PRESSURES

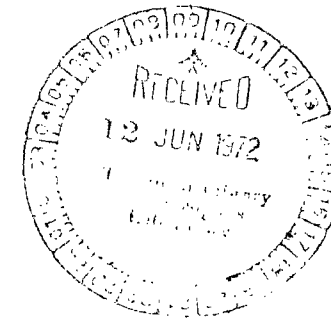

by Sherwood Hoffman

Langley Research Center
Hampton, Va. 23365

NATIONAL AERONAUTICS AND SPACE ADMINISTRATION • WASHINGTON, D. C. • JUNE 1972

1. Report No. NASA TN D-6817	2. Government Accession No.	3. Recipient's Catalog No.
4. Title and Subtitle NORMAL IMPINGEMENT LOADS DUE TO SMALL AIR JETS ISSUING FROM A BASE PLATE AND REFLECTING OFF A PLATFORM FOR VARIOUS JET MACH NUMBERS, SEPARATION DISTANCES, AND AMBIENT PRESSURES		5. Report Date June 1972 6. Performing Organization Code
7. Author(s) Sherwood Hoffman		8. Performing Organization Report No. L-8356
9. Performing Organization Name and Address NASA Langley Research Center Hampton, Va. 23365		10. Work Unit No. 117-07-04-10 11. Contract or Grant No.
12. Sponsoring Agency Name and Address National Aeronautics and Space Administration Washington, D.C. 20546		13. Type of Report and Period Covered Technical Note 14. Sponsoring Agency Code
15. Supplementary Notes		

16. Abstract

An investigation was conducted in the 12.5-meter-diameter vacuum sphere at the Langley Research Center to determine the impingement loads due to air jets issuing from and perpendicular to a circular base and reflecting off a square platform, that is, a simulation of rendezvous maneuvering, docking, launch, impact dampers, etc. The nozzles had exit Mach numbers of 1, 3, 5, and 7. The ambient pressures were 6×10^{-4}, 5, 225, and 760 torr. Under near-field separation distances and at 6×10^{-4} torr, reflections were significant; and ratios of the impingement force to thrust on both plates in the biplane arrangement varied from about 750 for exit Mach number 1 to 120 for exit Mach number 7. The far-field force ratios were near unity for the platform and zero for the base and indicated few, if any, reflections. Some reversals and rapid changes in loads were obtained at transition distances between the near and far fields. In general, increasing the exit Mach number or ambient pressure reduced the impingement loads.

17. Key Words (Suggested by Author(s)) Normal jet impingement Forces Nozzles Jet reflections	18. Distribution Statement Unclassified – Unlimited		
19. Security Classif. (of this report) Unclassified	20. Security Classif. (of this page) Unclassified	21. No. of Pages 23	22. Price* $3.00

*For sale by the National Technical Information Service, Springfield, Virginia 22151

NORMAL IMPINGEMENT LOADS DUE TO SMALL AIR JETS ISSUING FROM A BASE PLATE AND REFLECTING OFF A PLATFORM FOR VARIOUS JET MACH NUMBERS, SEPARATION DISTANCES, AND AMBIENT PRESSURES

By Sherwood Hoffman
Langley Research Center

SUMMARY

An investigation was conducted in the 12.5-meter-diameter vacuum sphere at the Langley Research Center to determine the static, normal impingement loads due to air jets issuing from and perpendicular to a circular base plate and reflecting off a square platform. Such information will be useful for studying configurations and procedures for landing, take-off, docking, and close maneuvering of spacecraft. The nozzles had nominal exit Mach numbers of 1, 3, 5, and 7. The normal separation distance between the plates varied from about 0 to 100 exit diameters. The ambient pressures were 6×10^{-4}, 5, 225, and 760 torr. (1 torr = 133.32 N/m^2.)

The variations of the ratio of normal force to thrust with plate separation distance were similar for all tests. The near-field load ratios on both the platform and the base in the biplane arrangement were large and constant for each case. At an ambient pressure of 6×10^{-4} torr, the ratio of force to thrust varied from about 750 for the Mach 1 nozzle to 120 for the Mach 7 nozzle for both reflecting surfaces. The far-field ratios of force to thrust also leveled off to constant values but of much lower magnitude. The latter varied from about 1.3 for a ratio of jet exit pressure to ambient pressure of 10^7 to about 0.8 for a ratio of 10^{-2}. The loads at the transition distances between the far and near fields experienced both load reversals and rapid changes in magnitude. Increasing the jet Mach number or ambient pressure generally reduced the magnitude of the ratios of impingement force to thrust. A comparison of the near-field results with and without base plate reflections indicated that the platform force-thrust ratio was increased by the multiwave reflections about 750:1 for Mach 1 and 2:1 for Mach 7 under near-vacuum ambient pressures and very small separation distances. For the far-field cases, where the plates experienced few, if any, reflections, there was little or no amplification of the loads.

INTRODUCTION

Under certain conditions the impingement loads from nozzle exhaust gases can damage the structural or mechanical parts of the spacecraft. Examples of these are given in the NASA space vehicle design criteria on staging loads (ref. 1). Also, as is shown in reference 2, the forces due to jet plume impingement may be significantly greater in a vacuum than in the atmosphere. In space the jet streamlines are straight lines that can undergo specular reflections off nearby surfaces. The resulting impingement load due to the change in momentum of the jet may be greater than the gross thrust of the isolated nozzle. There are operational situations in space when the jet streamlines would reflect many times to amplify the total impingement load affecting both the structure and maneuvering dynamics – for example, spacecraft decelerators operating during rendezvous, employment of impact dampers and air cushions between vehicles, and fire-in-the-hole staging. With some atmosphere present, on the other hand, the jet streamlines would turn and flow along the impingement surface to produce loads that are approximately equal to or less than the gross thrust.

A survey of the literature (ref. 3) showed that most of the jet-impingement studies made to date were concerned with pressures and temperatures. A few studies were made to measure the impingement loads on isolated flat plates, for example, reference 2 for normal jets and references 4 and 5 for parallel jets. The purpose of this investigation was to determine the jet-impingement loads for multireflected jets discharging normal to and between two parallel flat surfaces. The jet issued from the center of a circular base plate, impinged onto a large square platform, and was reflected back and forth between the plates. The distance between the plates was varied in a manner similar to docking or launch. It was anticipated also that the number of wave reflections between the plates would increase as the separation distance was reduced and thereby the loads would be increased to a comparatively high magnitude. The nozzles were tested with air and had nominal exit Mach numbers of 1, 3, 5, and 7. Four ambient pressures were employed: (1) near vacuum, (2) earth pressure altitude of 34 km (estimated Martian surface pressure), (3) earth pressure altitude of 9 km, and (4) earth sea level. All the tests were conducted in the 12.5-meter-diameter vacuum sphere at the Langley Research Center.

SYMBOLS

The axis system, dimension nomenclature, and force relationships are illustrated in figure 1.

A_j area of nozzle exit

d_j	diameter of nozzle exit
d_t	diameter of nozzle throat
F_N	static force on flat plate, normal to surface
H	normal distance between flat plates
M_j	jet-exit Mach number
$\dot{m}$	mass flow
p_a	ambient pressure in vacuum sphere
p_{ch}	total pressure or chamber pressure of nozzles
p_j	nozzle-exit static pressure
R	nozzle-exit Reynolds number, based on d_j
T_j	vacuum gross thrust of nozzle
V_j	jet exit velocity
α_n	initial jet turning angle measured between nozzle center line and tangent to jet boundary at nozzle lip
γ	ratio of specific heats, 1.40 for air
θ_n	nozzle half-angle
ν_n	Prandtl-Meyer expansion angle from sonic velocity to nozzle-exit Mach number
ν_1	Prandtl-Meyer expansion angle from sonic velocity to jet-boundary Mach number

APPARATUS

A schematic diagram and a photograph of the apparatus are shown in figures 1 and 2. The apparatus consisted of two flat plates, two strain-gage force balances, two dashpots, four different nozzles, two plenum chamber pressure gages, and a remotely controlled test stand and air supply. The square platform had a smooth surface with dimensions of 61.0 cm on each side and could be considered as either a launching platform or the docking surface of a target vehicle. The round or disk base plate also had a flat smooth surface and a diameter of 30.5 cm. This base plate had a 5.08-cm hole at its center for the nozzle. The space between the nozzle circumference and hole edge was adjusted to give a clearance of 0.32 cm (fig. 1(a)). The nozzle and base plate arrangement could be considered as a launch vehicle base section or the docking surface of an approach vehicle. Both plates were rigid and were constructed to be within the weight allowances of the balances.

The basic dimensions and characteristics of the nozzles are given in figure 1(b). The isentropic, jet exit Mach numbers of the conical nozzles were based on the actual area ratios of the nozzles, by using data from reference 6, and differed slightly from the nominal Mach numbers. All the nozzles had about the same throat area. The exit plane of each nozzle was alined with the surface of the base plate which faced the platform. Air was supplied to the nozzles by means of a pressure regulator and quick opening valve located near the center of the vacuum sphere. This arrangement provided accurate control of the nozzle plenum chamber pressure for each test run. The chamber pressures were measured with a Statham pressure gage for most of the cases and a differential pressure gage for the very low pressures. The stagnation temperature in the gas supply accumulator was measured by a thermocouple.

TESTS AND MEASUREMENTS

The tests were conducted in the 12.5-meter vacuum sphere at the Langley Research Center. The parameters varied are summarized in table I and were (1) nozzle exit Mach number M_j, (2) separation or normal distance H between the plates, and (3) ambient pressure p_a (measured on wall of vacuum sphere). The perpendicular distance between the plates, measured in terms of nozzle exit diameters, varied from about 0 to 100. An additional displacement of any one plate due to loading of the balances was determined experimentally to be about 10^{-4} cm and was neglected. The reference height of zero was obtained by pressing the two planes together until each balance had a static load or bias of about 0.1 kg. Zero height or separation distance was never obtained because air continued to escape from the rim of the nozzle and between the plates at contact. Therefore, all zero-height data were plotted at $H/d_j = 0.001$ for convenience. Some vertical

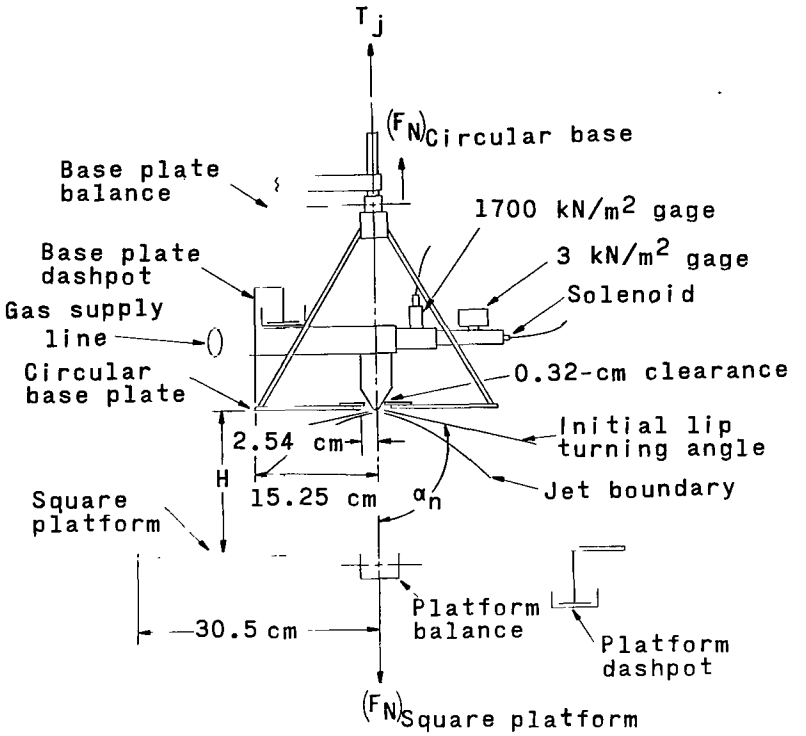

(a) Nozzle and plate assembly.

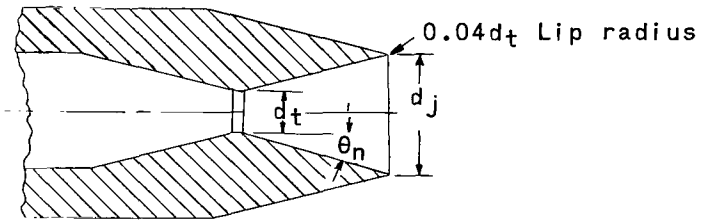

M_j (nominal)	M_j (isentropic)	d_t, cm	d_j, cm	θ_n, deg	γ
1	1.00	0.318	0.318	0	1.40
3	2.95	.318	.640	15	1.40
5	4.93	.327	1.588	15	1.40
7	6.95	.320	3.213	18.3	1.40

(b) Nozzle characteristics.

Figure 1.- Schematic representation of apparatus.

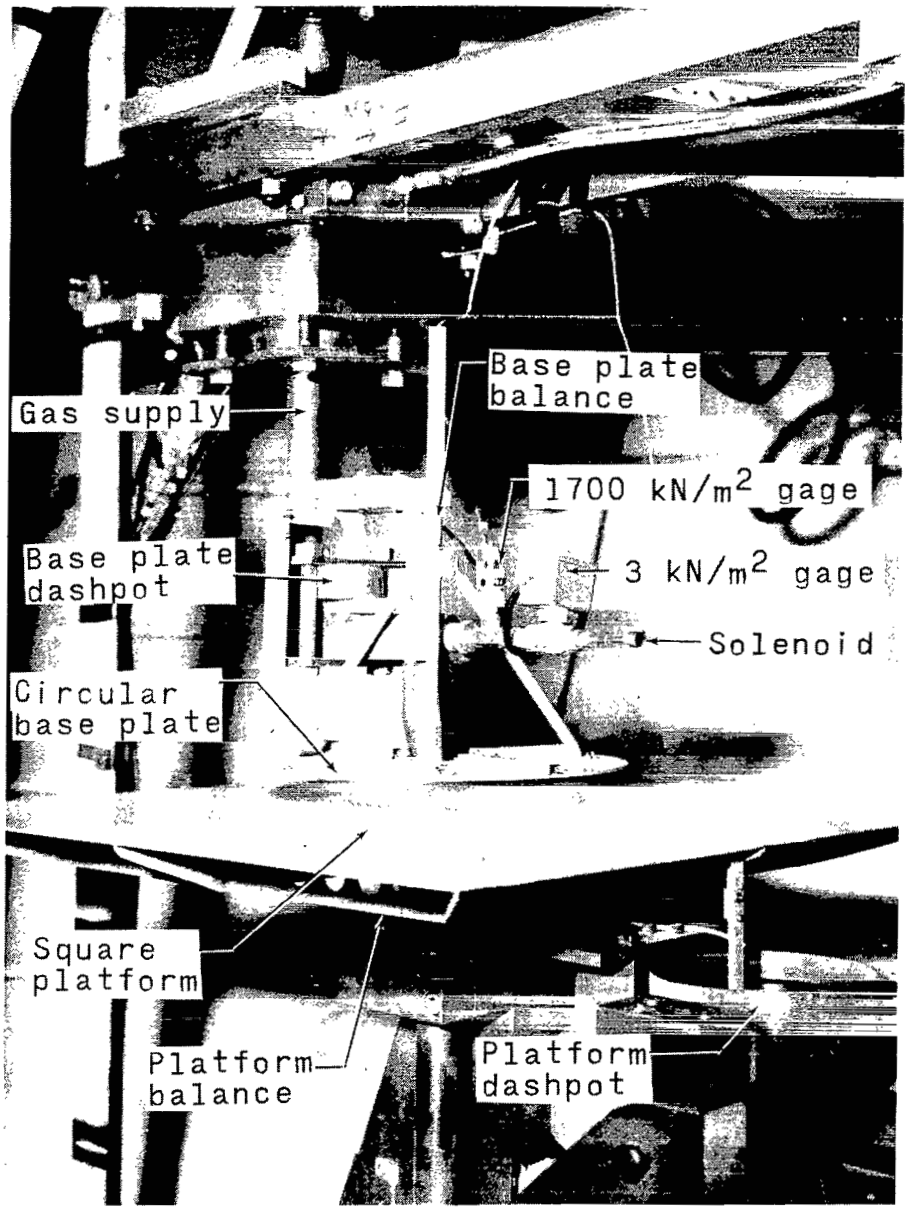

L-71-6636.1

Figure 2.- Photograph of apparatus.

TABLE I.- CHAMBER PRESSURES

Height		p_{ch}, torr, at ambient pressure, p_a, torr, of –			
H, cm	$\frac{H}{d_j}$	6×10^{-4}	5	225	760
		$M_j = 1.00$			
0	0	22.6	48	539	301.5
.0051	.016	22.6	48	512	356
.0127	.040	21.5	47	593	410
.0178	.056	21.5	47	539	411
.0254	.080	20.4	46	458	411
.0508	.160	20.4	46	485	410
.0762	.240	1 934	46	970	1 150
					2 542
.1016	.328	20.4	44	2 371	3 812
.1219	.384	-------	-------	------	4 958
.1270	.400	19.3	142	2 371	4 892
					3 750
.1575	.496	20.4	140	2 263	3 496
.3175	1.0	19.3	204	2 156	3 623
		96.7	3 367		
			5 973		
.635	2.0	196	3 687	2 048	3 559
		6 938	8 833		
1.270	4.0	11 922	8 580	4 322	7 437
1.905	6.0	14 067	8 389	6 611	7 375
2.540	8.0	8 958	11 631	6 801	7 499
		5 760	7 818	7 824	9 725
5.080	16	5 635	7 818	7 698	9 789
7.620	24	5 572	7 944	7 824	9 789
10.160	32	5 509	7 882	7 698	9 534
12.700	40	5 635	7 944	7 571	9 789
15.240	48	10 850	10 643	10 850	9 935
20.320	64	10 881	10 706	10 724	9 935
25.400	80	10 850	10 768	10 660	9 935
30.480	96	10 845	10 706	10 661	9 966
		$M_j = 2.95$			
0	0	47.3	86.9	539	784
.0051	.0079	47.3	84.8	539	739
.0127	.0198	46.2	82.7	512	730
.0178	.0277	46.2	80.7	539	677
.0254	.0395	45.2	82.2	539	622
.0508	.0791	44.1	76.5	566	568
.0762	.1186	44.1	75.5	539	2 027
					2 947
					3 812
					5 163
.1016	.1581	43.0	197	539	5 163
				1 644	
.1270	.1976	43	190.3	1 752	5 161
				1 698	
.1575	.2451	43	187.2	-----	5 110
					3 163
.3175	.4941	41.9	752	1 617	3 190
			1 424		
.6350	.9881	147	2 340	1 536	3 109
		193	3 465	3 099	-----
		402	5 721	-----	-----
		750	5 721	-----	-----
1.270	1.976	1874	5 396	4 500	3 082
1.905	2.964	3641	5 506	4 473	5 298
2.540	3.953	5971	5 264	5 659	6 353
		5677	10 426	5 614	6 229
			10 424		
5.080	7.91	5488	12 013	9 021	6 229
					8 771
					9 852
7.620	11.86	8200	11 886	11 418	11 187
10.160	15.81	8011	11 886	11 354	11 250
12.700	19.76	8011	11 886	11 292	11 250
15.240	23.72	8011	11 886	11 292	11 123
		7818	11 480	11 440	10 742
20.320	31.62	7691	11 480	11 505	10 742
25.400	39.53	7818	11 480	11 505	10 742
30.480	47.43	7691	11 543	11 505	10 742

Height		p_{ch}, torr, at ambient pressure, p_a, torr, of –			
H, cm	$\frac{H}{d_j}$	6×10^{-4}	5	225	760
		$M_j = 4.93$			
0	0	49.5	101.9	751	626
		27			
.0051	.0032	26	103.5	751	814
.0127	.0080	26	103.5	751	-------
.0178	.0112	25	100.3	689	876
.0254	.0160	25	100.3	689	938
					2 629
.0508	.0320	25	98.8	689	2 692
.0762	.0480	26	98.8	689	2 629
.1016	.0640	24	98.8	1 002	2 567
.1270	.0800	43	294	2 629	2 567
.1575	.0992	124	286.5	2 880	2 442
.3175	.200	124	272.6	2 942	4 758
			487		
			757		
.6350	.400	199	1 027	3 130	4 695
					8 076
1.270	.800	754	1 244	5 509	8 076
1.905	1.200	3233	3 271	5 071	7 826
2.540	1.6	3072	3 298	6 887	7 701
	1.6	5572	8 136	8 011	7 888
					7 074
					7 387
5.080	3.2	5447	8 390	8 074	7 200
					7 450
7.620	4.8	5572	8 263	8 011	7 638
					7 575
10.160	6.4	5634	7 945	8 011	7 074
					7 450
12.700	8.0	6824	8 072	8 011	7 137
					7 513
15.240	9.6	5447	8 013	10 205	9 579
20.320	12.8	5447	7 951	10 267	9 829
25.400	16.0	5384	7 951	10 267	9 704
30.480	19.2	5447	7 826	10 017	9 766
		$M_j = 6.95$			
0	0	44	269	510	775.8
			81		1 427
			89		539.0
.0051	.00158	48	88	564	538.9
.0127	.0040	41	83	537	458.2
.0178	.0055	42	72	564	431.3
.0254	.0079	40	97	591	404.4
.0508	.0158	40	117	564	323.2
.0762	.0237	31	137	564	1 186
				1 986	
				3 623	
				4 541	
				5 990	
.1016	.0316	37	158	6 098	2 156
					3 934
.1270	.0395	36	116	6 046	3 961
				3 196	
.1575	.0490	33	188	3 384	3 907
.3175	.0988	45	177	3 438	3 880
			566		
			727		
			2 371		
.6350	.1976	145	2 182	3 411	3 853
	.1976	193	2 075		
	.1976	803			
1.270	.395	2034	2 121	3 331	6 387
1.905	.593	4846	3 665	3 384	6 387
					8 515
2.540	.791	4819	6 009	5 694	8 461
	.791	5720	5 741	5 721	7 246
5.080	1.58	5658	5 741	5 721	7 308
7.620	2.37	5720	5 741	5 784	7 375
10.160	3.16	5720	5 803	5 784	7 308
12.700	3.95	5658	5 549	5 658	7 500
16.510	5.14	5173	10 742	10 613	10 859
20.320	6.32	5048	10 680	10 613	10 359
25.400	7.91	5048	10 742	10 680	16 715
30.480	9.49	5048	10 612	10 550	10 488
45.720	14.23	----	10 845	10 760	10 054
59.690	18.58	----	11 099	10 954	10 183

positions were repeated at different chamber pressures, as may be observed in the table. These positions were limited to regions where the force measurements changed rapidly with vertical displacement.

The four nozzles had nominal exit Mach numbers of 1, 3, 5, and 7. The air supplied was dry (-70° C frost point maximum); nevertheless, according to reference 7, the Mach 5 and 7 nozzles were operating under saturation temperatures and pressures. As a consequence of some liquefaction, they may have had a 10-percent reduction in exit Mach number. The ambient pressure was constant for each series of Mach number and distance tests. The four ambient pressures selected, 6×10^{-4} torr, 5 torr, 225 torr, and 760 torr, corresponded to earth pressure altitudes of about 94 km, 34 km, 9 km, and sea level, respectively. (1 torr = 133.32 N/m^2.) The nozzle chamber pressure was constant for each test. The chamber pressures were varied between tests (table I) because lower chamber pressures were required at the small separation distances $\left(H/d_j < 1\right)$ in order not to overload the balances.

Two three-component balances were used to measure the forces on the plates. They were located along the vertical axis of symmetry of each plate since only the normal force was of interest in this investigation. The normal-force range of each balance was ±2.5 kg.

The nozzle gross thrusts, exit pressures, and Mach numbers were computed for isentropic flow (ref. 6) in a vacuum, corrections for exit flow divergence and discharge coefficient (ref. 8) being neglected, as follows:

$$T_j = \dot{m}V_j + p_jA_j = p_{ch}A_j\left(\frac{p_j}{p_{ch}}\right)\left(1 + \gamma M_j^2\right)$$

and

$$p_j = p_{ch}\left(1 + \frac{\gamma - 1}{2} M_j^2\right)^{-\frac{\gamma}{\gamma-1}}$$

The nozzles were highly underexpanded when operating at ambient pressures of 6×10^{-4} torr. The jet lip turning angles as a function of the ratio of jet-exit static pressure to ambient pressure for the nozzles tested at 6×10^{-4} torr are shown in figure 3. These angles, obtained from the expression $\alpha_n = \nu_1 - \nu_n + \theta_n$, are shown in figure 3 to be close to the turning angles for a vacuum. At higher ambient pressures the nozzles were tested with either overexpanded flow or underexpanded flow because of the constraints imposed on the chamber pressures by the balances.

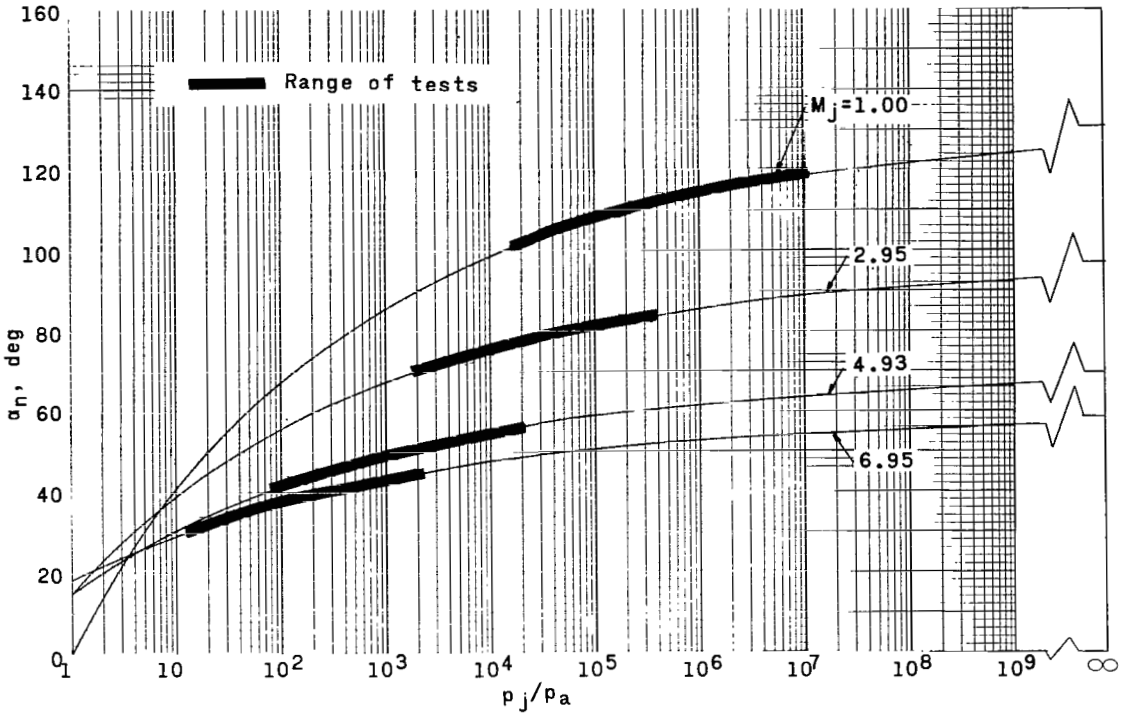

Figure 3.- Variation of initial turning angle with ratio of jet-exit pressure to ambient pressure for nozzles tested with underexpanded flow at a sphere pressure of 6×10^{-4} torr.

Typical measurements with their accuracies, based on instrument accuracies, are summarized as follows:

F_N, kg	2.5 ± 0.03
p_{ch}, torr	$13\,000 \pm 150$
p_{ch}, torr	200 ± 3
p_a, torr	$(6 \times 10^{-4}) \pm (6 \times 10^{-5})$
p_a, torr	5 ± 0.1
p_a, torr	225 ± 1
p_a, torr	760 ± 1
H, cm:	
0.16 to 15	$\pm 2 \times 10^{-3}$
0 to 0.16	$\pm 5 \times 10^{-4}$

There are other sources of error which may be significant when the plate separation distances are small, such as inaccuracies due to the lack of knowledge of true exit Mach number and separation of the flow inside the nozzle.

RESULTS AND DISCUSSION

Basic Data

A sample oscillograph record is presented in figure 4 to show the traces of normal force and nozzle chamber pressure for a typical run. The axial force and pitching moment were essentially zero for all runs and are not shown on the sample record. The data points were read where the traces were nearly constant at 0.05 second before the end of each test. The average running time for a test was about 0.25 second.

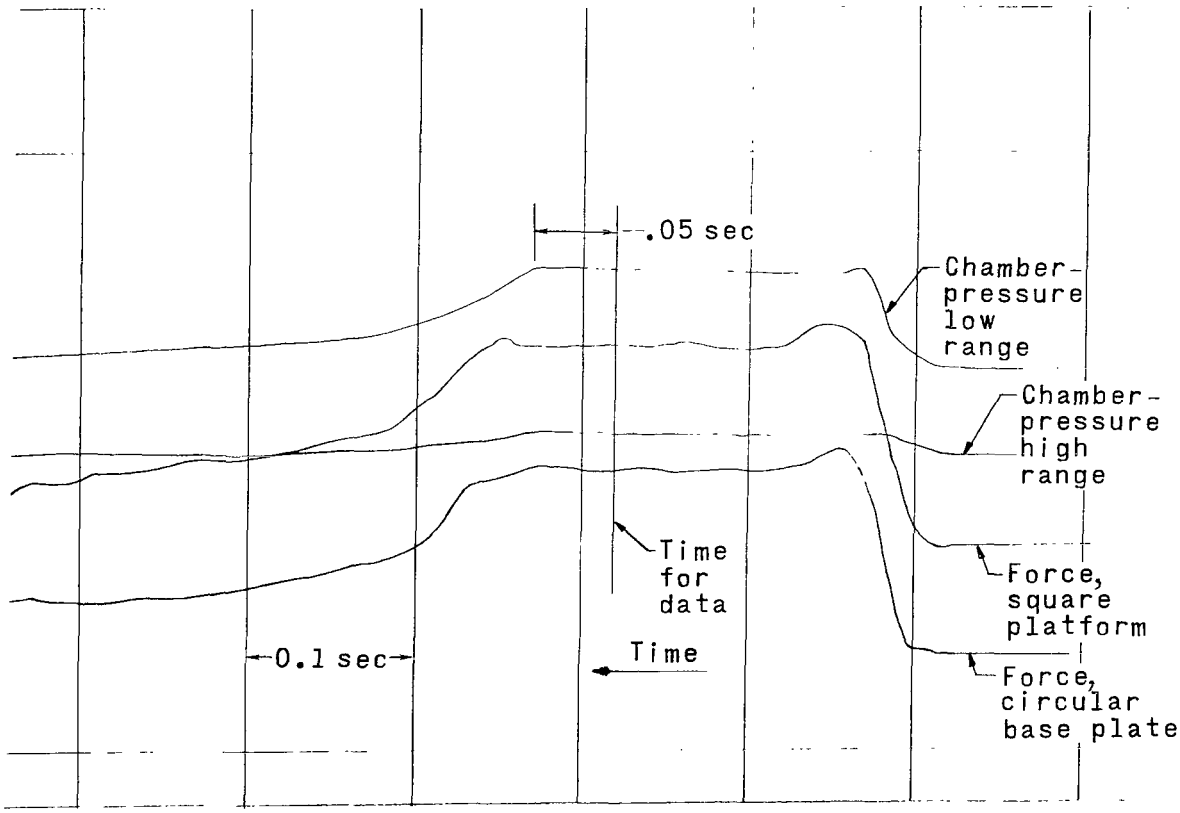

Figure 4.- Typical oscillograph record.

The force data, the separation distances, and nozzle-exit static pressures were nondimensionalized by dividing by values of computed gross thrust, nozzle-exit diameter, and ambient pressure, respectively. It can be seen from the values of chamber pressure presented in table I that some nozzles were investigated more than once by using different levels of pressure. The drop in p_{ch}, required by the balance limit, provided data which indicated that the parameter F_N/T_j had little or no dependence on mass flow rates or jet-exit Reynolds numbers for the ranges covered. The Reynolds numbers, based on respective exit diameters, are presented in figure 5. Two ranges of R are shown for

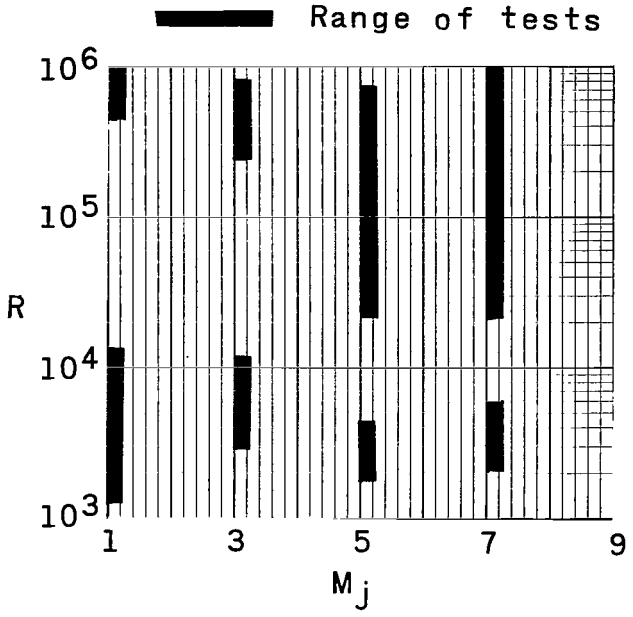

Figure 5.- Comparison of jet-exit Reynolds numbers for the nozzles. Reynolds numbers are based on exit diameters.

each nozzle, the high ranges corresponding to the higher chamber pressures and larger separation distances. For the high Reynolds number tests, reference 8 shows that the nozzle discharge coefficients would be near unity and can be neglected in computing thrust. The discharge coefficients for the lowest Reynolds numbers are about 0.95 and, also, are neglected for the comparisons.

General Results

The variations of normal-force ratio with vertical separation distance of the plates and for all the nozzles tested are presented in figures 6 to 9. The force ratios for the square platform alone, as obtained from reference 2, are also presented in these figures. This ratio was biased by ten $\left(\left(F_N/T_j\right) + 10\right)$ so that all the data, some of which had negative values at certain heights, could be summarized for each test run on log-log paper. A comparison of these figures shows that all the trends are similar and that the data can be separated into two groups, as in reference 2, to near-field and far-field regions. In general, the square platform loads are slightly higher than those of the circular base when tested together at corresponding values of H/d_j. This effect is probably due largely to the fact that the jets impinge on the platform first. Since the load ratios of the plates are nearly equal and the platform area is five times larger than the base area, it is evident that most of the loading occurs under the area covered by the smaller base plate.

The near-field and far-field loads are constant at their respective levels, but their magnitudes differ markedly. The comparisons in figures 6 to 9 show that the near-field

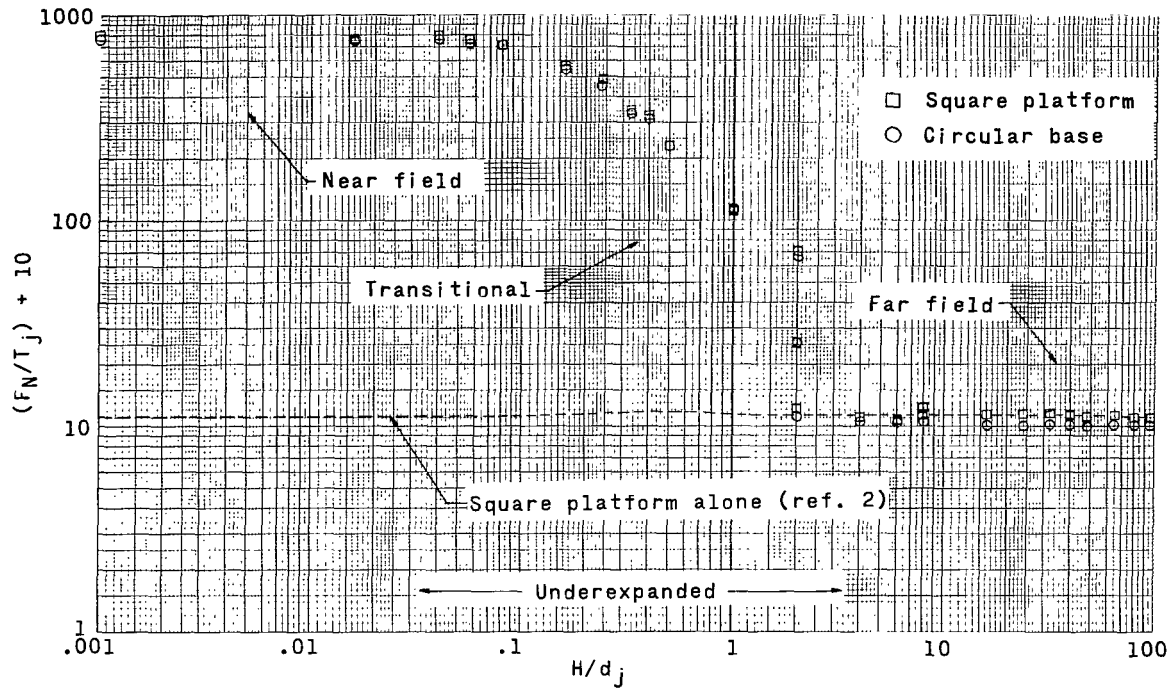

(a) Ambient pressure, 6×10^{-4} torr.

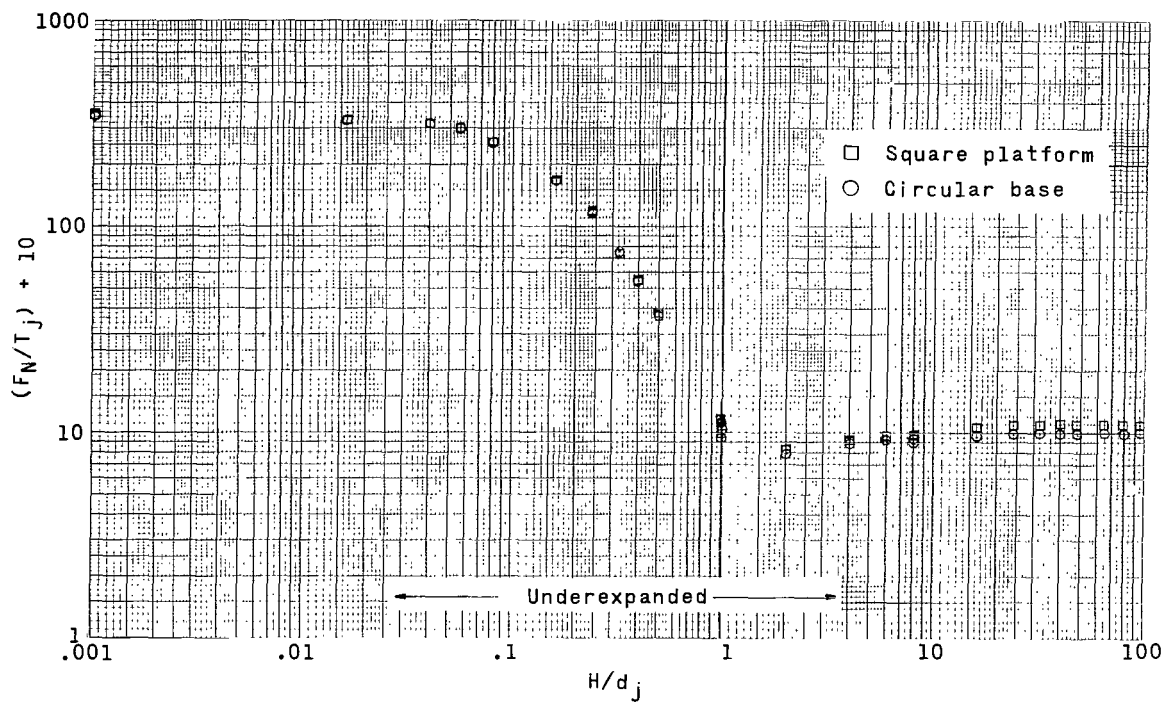

(b) Ambient pressure, 5 torr.

Figure 6.- Variations of ratio of normal force to thrust with separation distance between the plates for $M_j = 1.0$.

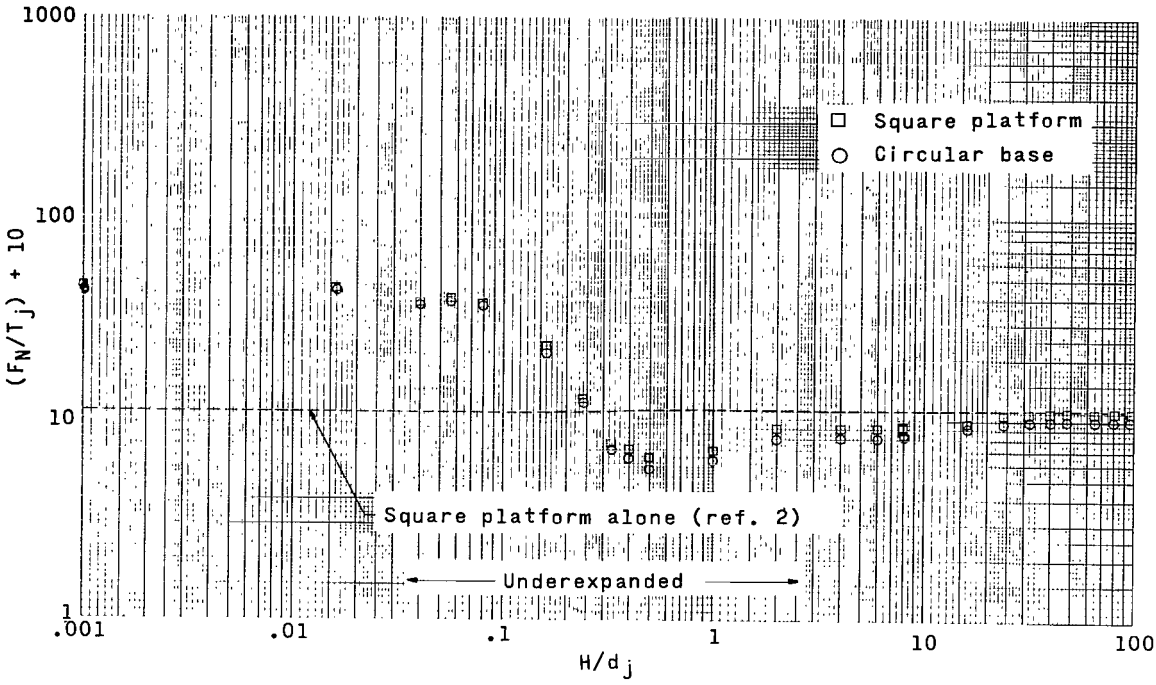

(c) Ambient pressure, 225 torr.

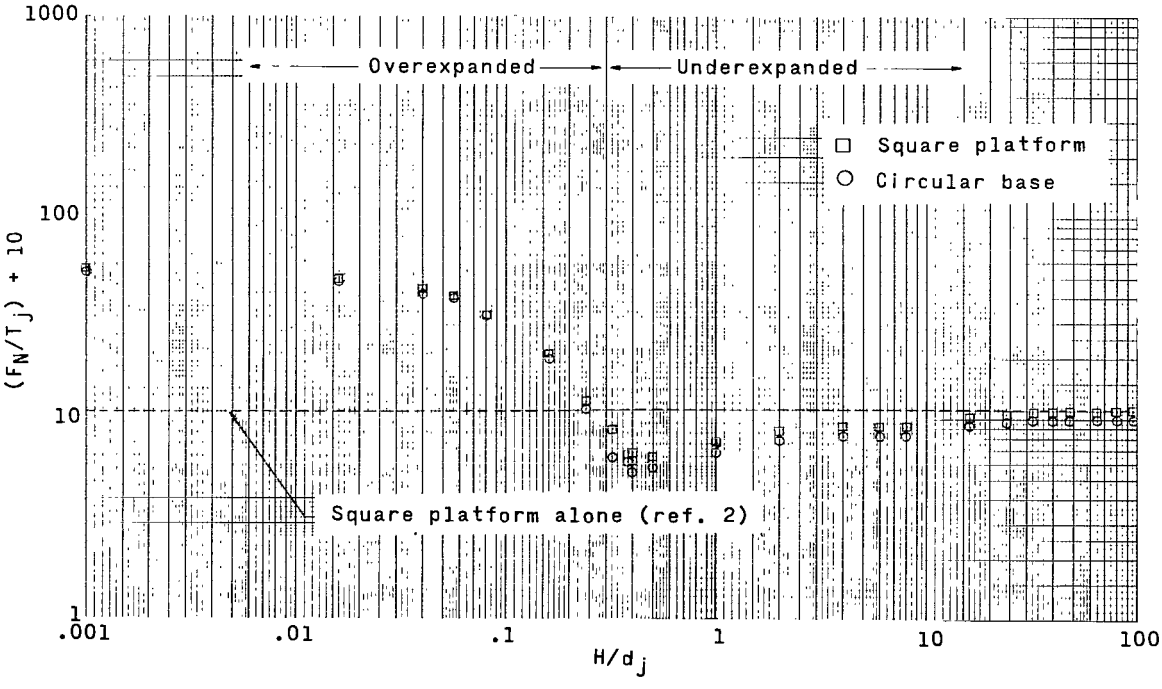

(d) Ambient pressure, 760 torr.

Figure 6.- Concluded.

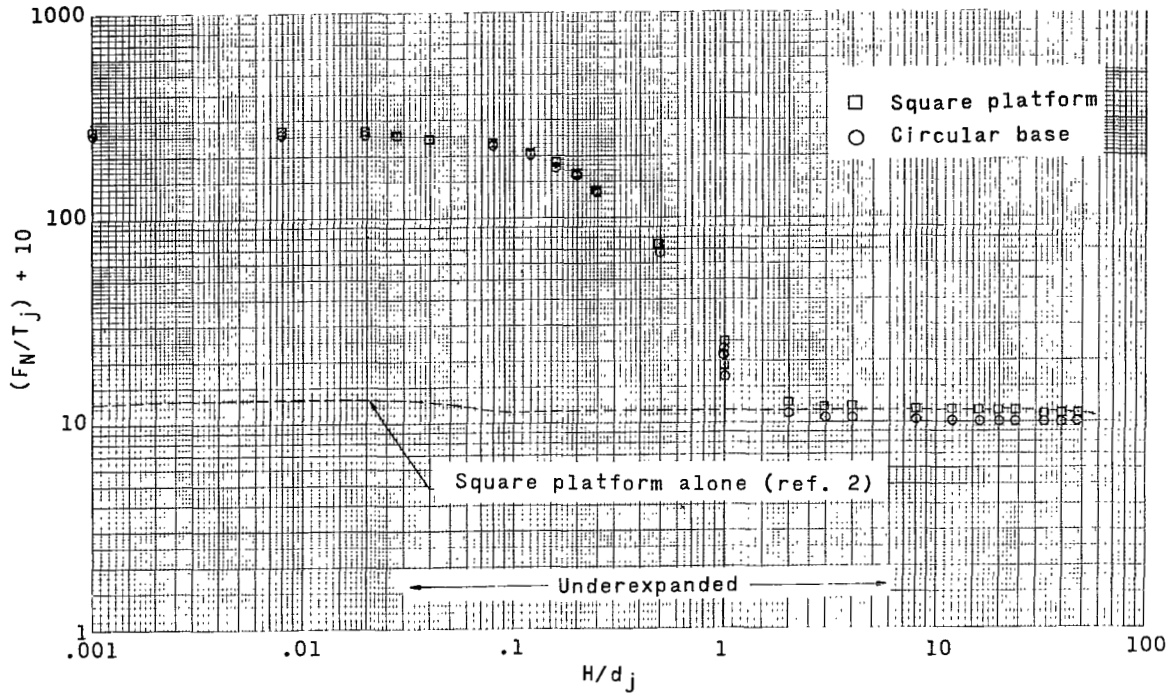

(a) Ambient pressure, 6×10^{-4} torr.

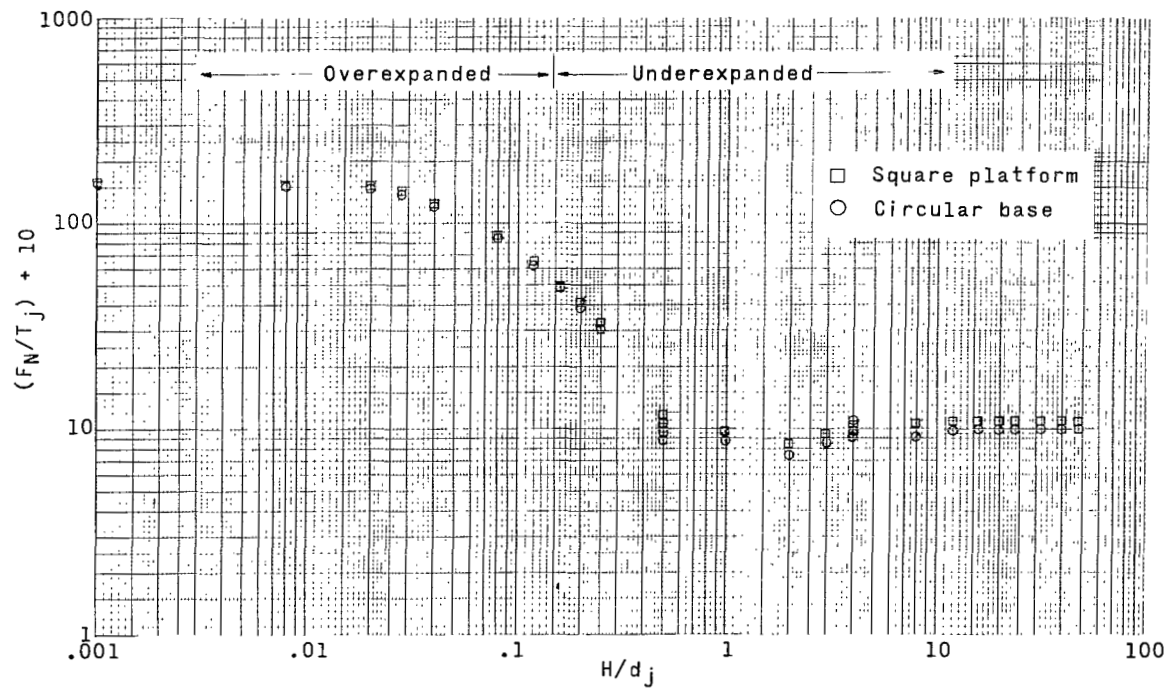

(b) Ambient pressure, 5 torr.

Figure 7.- Variations of ratio of normal force to thrust with separation distance between the plates for $M_j = 2.95$.

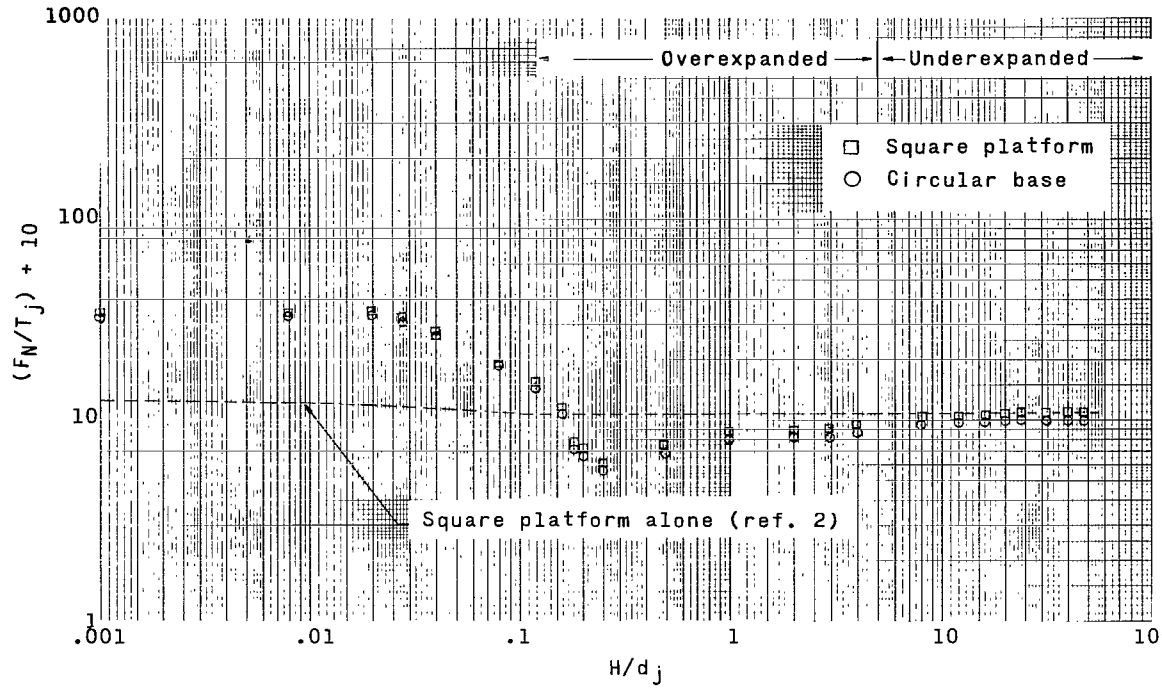

(c) Ambient pressure, 225 torr.

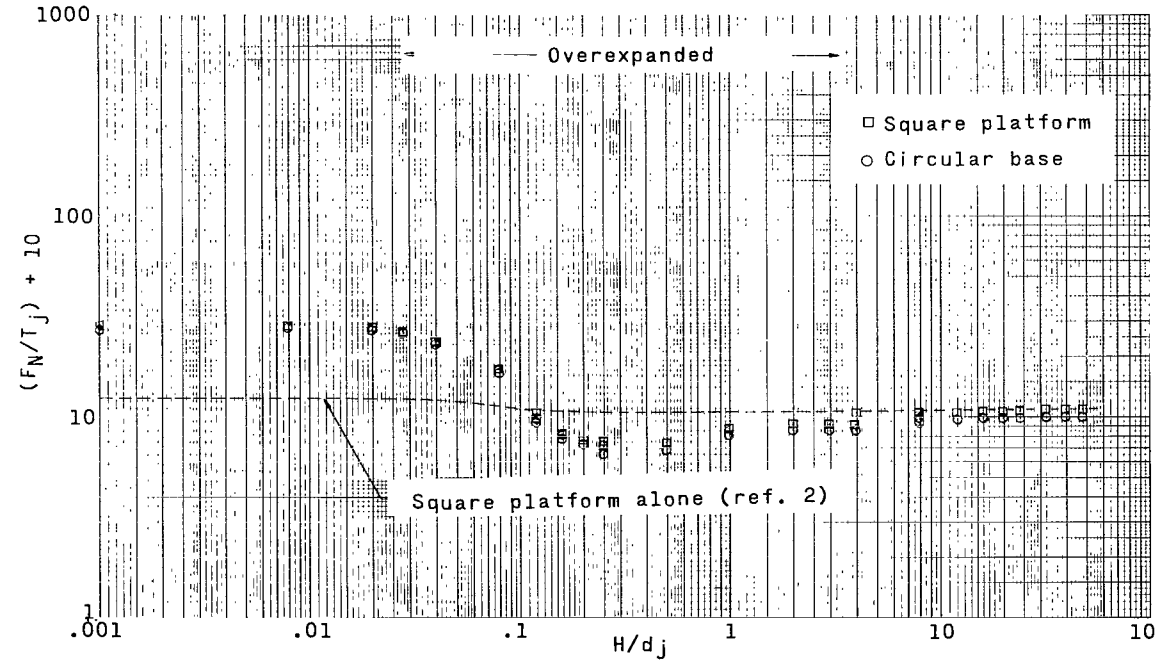

(d) Ambient pressure, 760 torr.

Figure 7.- Concluded.

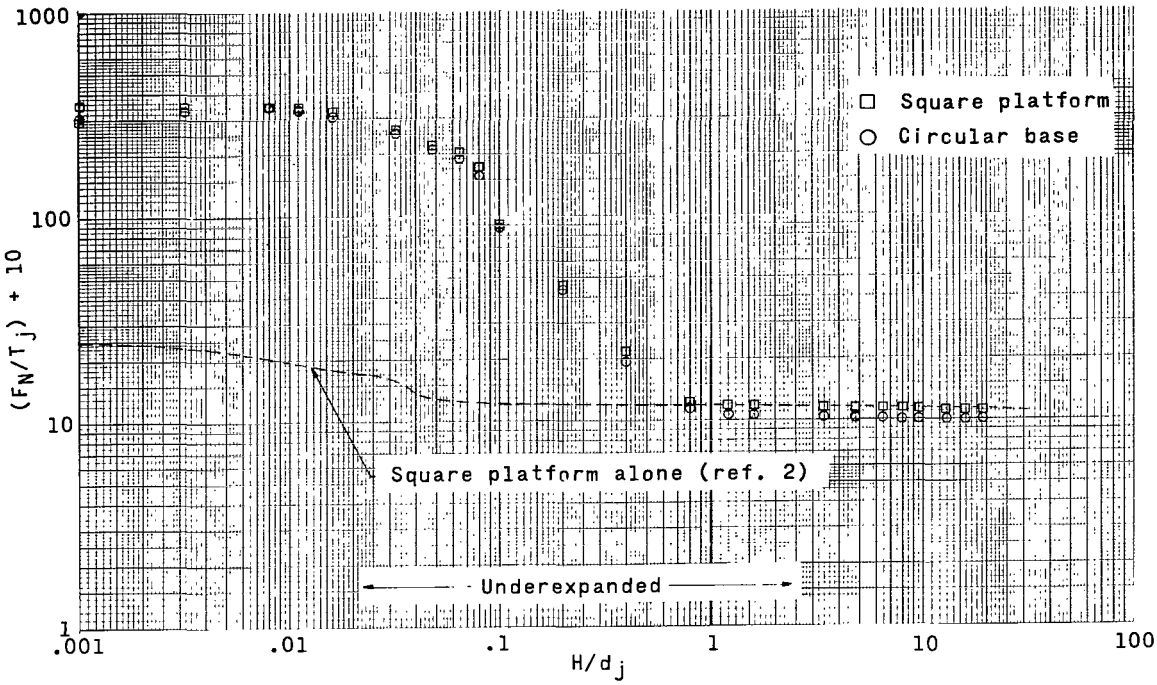

(a) Ambient pressure, 6×10^{-4} torr.

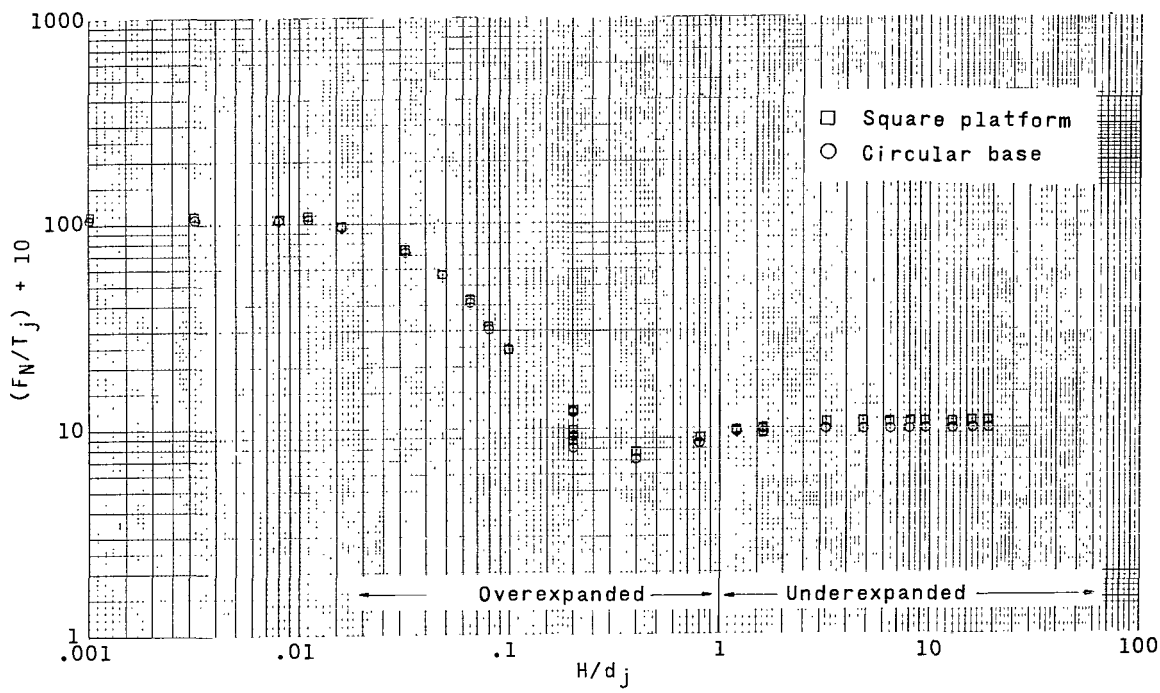

(b) Ambient pressure, 5 torr.

Figure 8.- Variations of ratio of normal force to thrust with separation distance between the plates for $M_j = 4.93$.

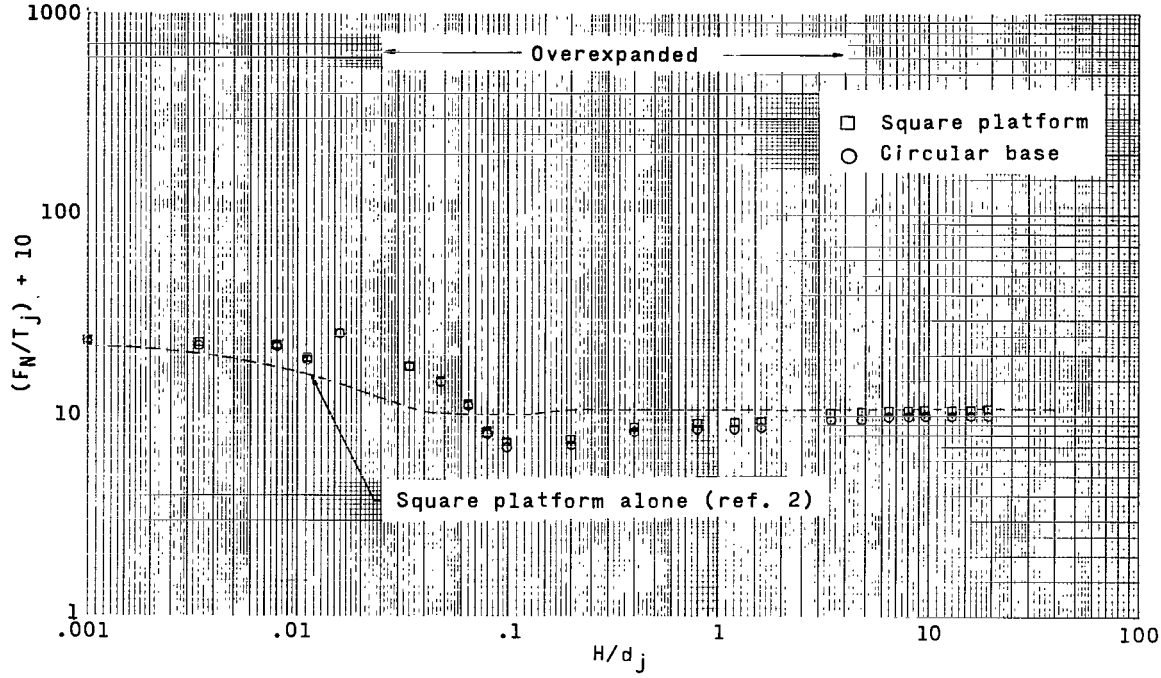

(c) Ambient pressure, 225 torr.

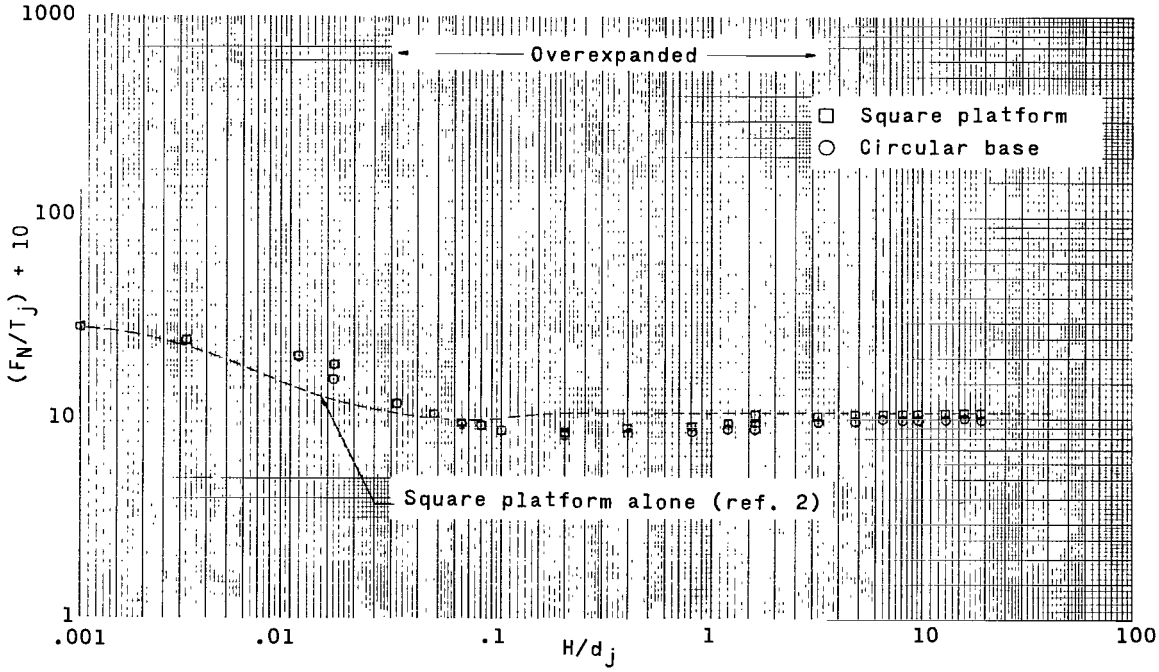

(d) Ambient pressure, 760 torr.

Figure 8.- Concluded.

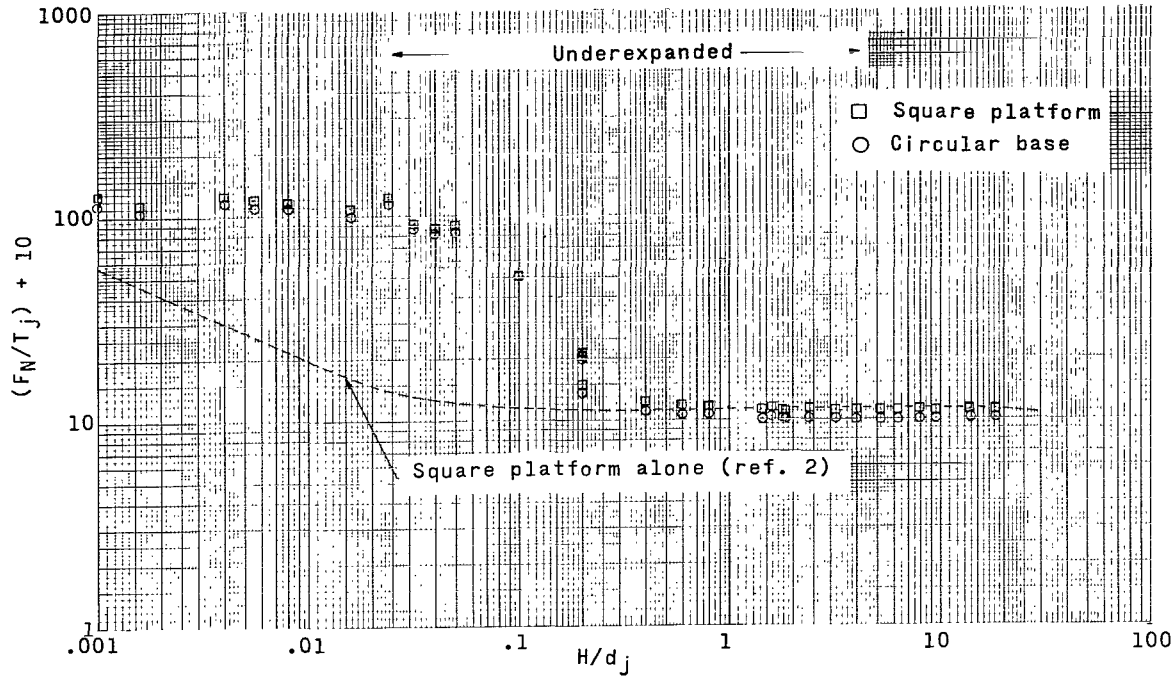

(a) Ambient pressure, 6×10^{-4} torr.

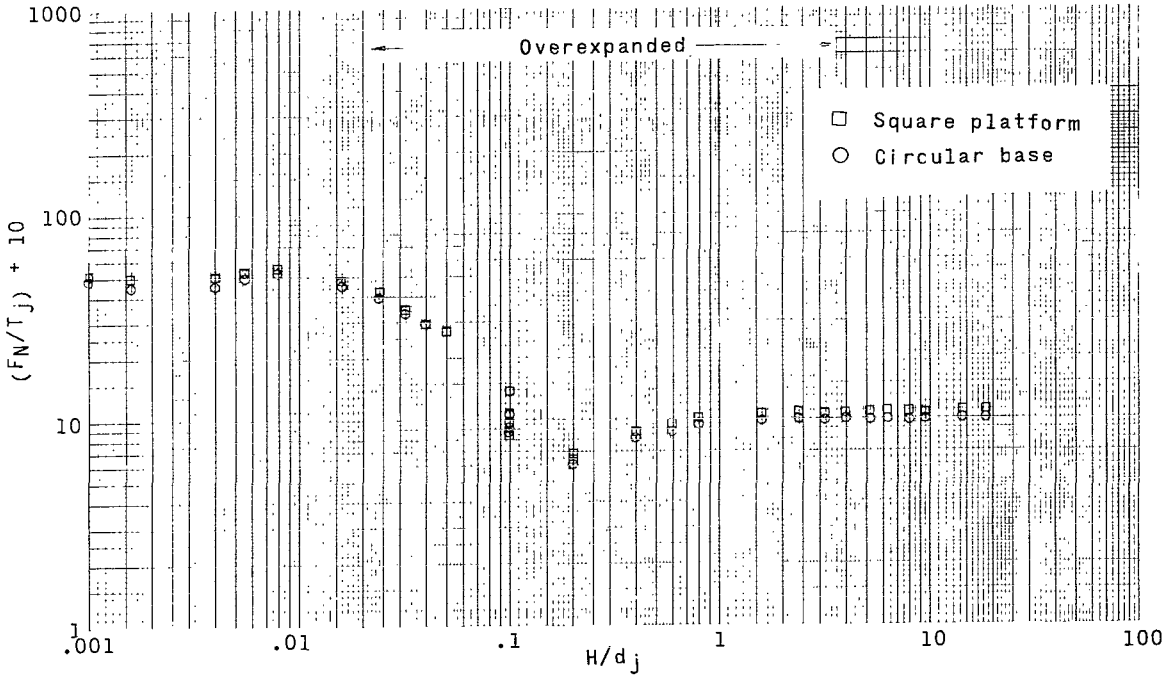

(b) Ambient pressure, 5 torr.

Figure 9.- Variations of ratio of normal force to thrust with separation distance between the plates for $M_j = 6.95$.

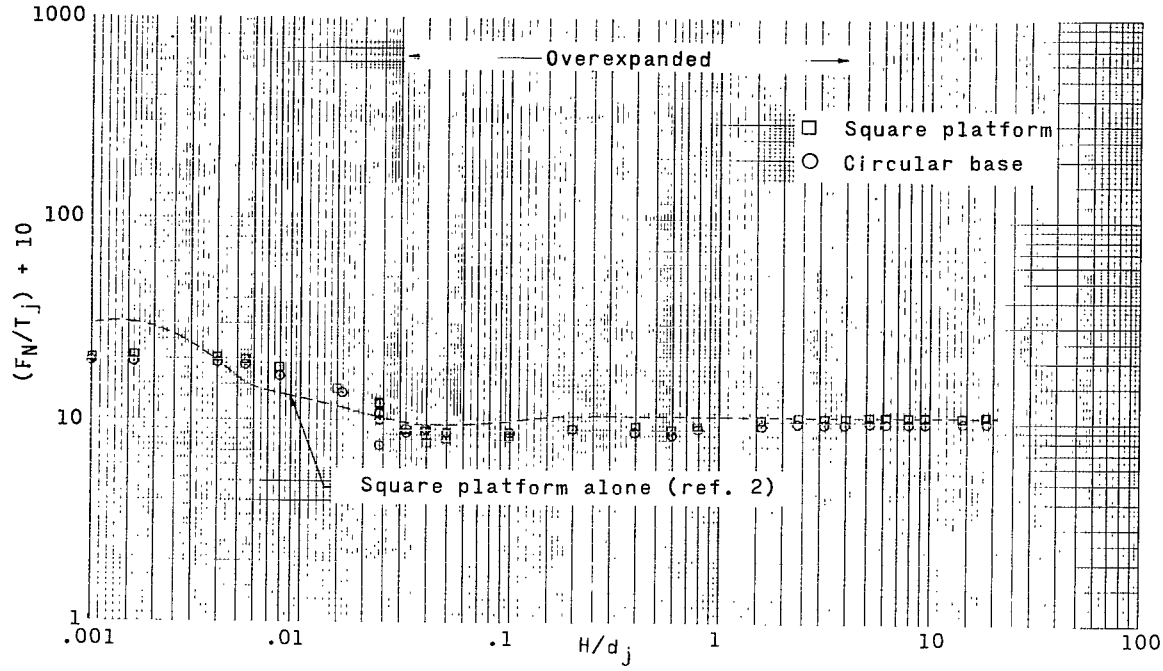

(c) Ambient pressure, 225 torr.

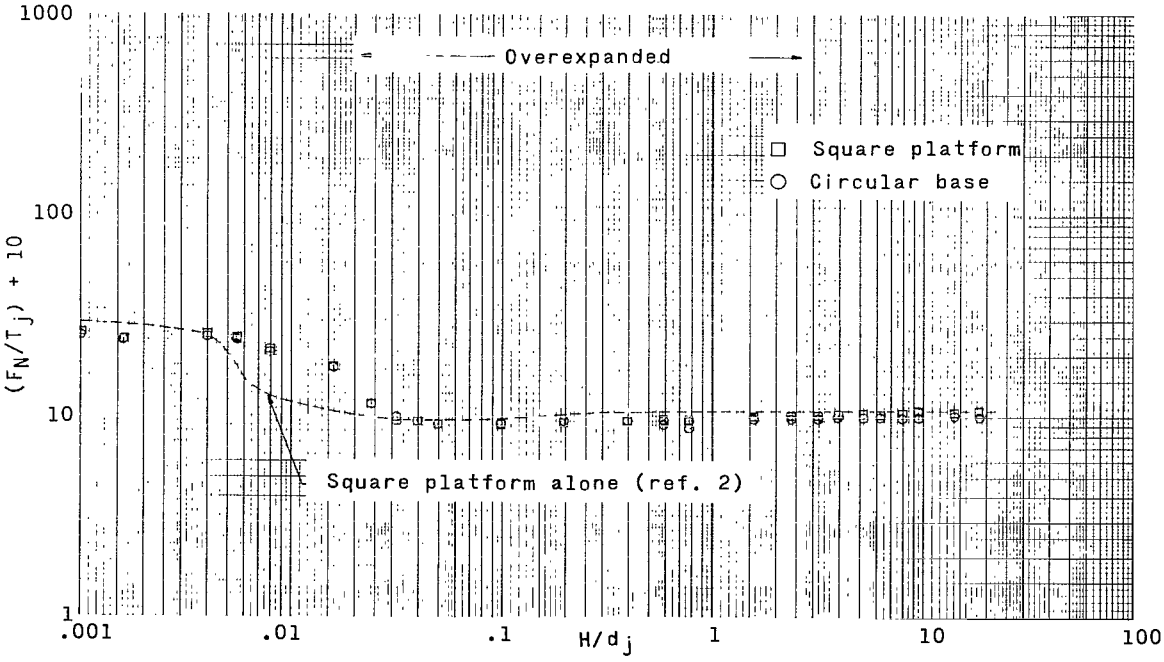

(d) Ambient pressure, 760 torr.

Figure 9.- Concluded.

loads are always larger than the corresponding far-field loads and that the two fields are joined by abrupt changes of loads at intermediate or transition heights. The large values of F_N/T_j obtained when the plates were very close are probably due to reflections and shocks in space and shocks in the atmosphere. There is a rapid falloff of impingement loads as the distance between the plates is increased. For the atmospheric tests (5 torr, 225 torr, and 760 torr) load reversals are obtained in the transition region; these reversals indicate aerodynamic lift on each plate. The plate loads then level off as the distance is increased further.

Far-Field Displacements

A correlation of the average loads from both the overexpanded and underexpanded nozzles is presented in figure 10 for far-field displacements of $10d_j$ or greater. At these heights, the two plates appear to be free of mutual interference effects and have load ratios of the same order of magnitude as the platform alone (ref. 2). For all practical purposes, the reflected load on the circular base is negligible or zero. This result was not surprising because the plates were too far apart for multireflections to occur. However, the impingement load to thrust ratio on the platform of the biplane arrangement varies from about 1.3 at $p_j/p_a = 10^7$ to about 0.8 at $p_j/p_a = 10^{-2}$. Under near-vacuum conditions, $p_j/p_a = 10^7$, the reflection angles of the streamlines varied between 90^o and 180^o on the platforms (ref. 2). If all the streamlines would have impinged normal to the platform, F_N/T_j would theoretically approach 2.0. The amount of scatter about the mean curves may have been due to such effects as variations of jet flow turning angle with pressure ratio, spillage off the plate, and experimental error. A comparison of these average

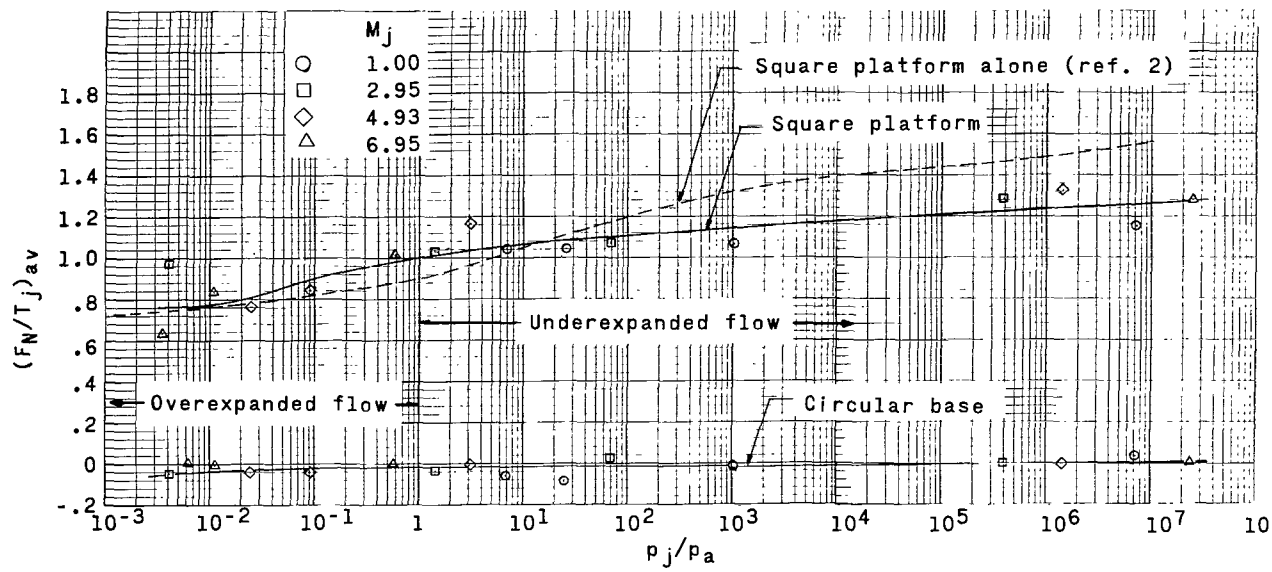

Figure 10.- Variation of ratio of average normal force to thrust with the ratio of jet pressure to ambient pressure for the far-field tests $\left(H/d_j \geq 10\right)$ of each nozzle.

ratios with those of the platform alone (ref. 2) shows that the far-field loads on the platform with reflections are slightly lower than those of the isolated platform for underexpanded nozzles and about equal for overexpanded nozzles. The effect of reflections on loads of parallel plates relatively far apart are small and negligible, for all practical design purposes.

Near-Field Displacements

The most interesting results obtained were the load amplifications which occurred within the near-field separation distances. At these small distances, the plates were very close and multireflections of waves were expected in a vacuum. As the separation distance approached zero, the loads increased rapidly and it was necessary to reduce considerably the nozzle chamber pressure to avoid overloading the balances. The low-range chamber pressure gage was used at these times to preserve the accuracy in computing gross thrust. The results obtained at zero height were the largest in magnitude and, therefore, represent maximum loads for the design of certain systems such as impact dampers.

The maximum or touchdown force to thrust ratios of the square platform are plotted in figure 11 against the maximum force parameter for all jet Mach numbers and altitudes. The values of F_N/T_j under near-vacuum ambient conditions (6×10^{-4} torr) were the

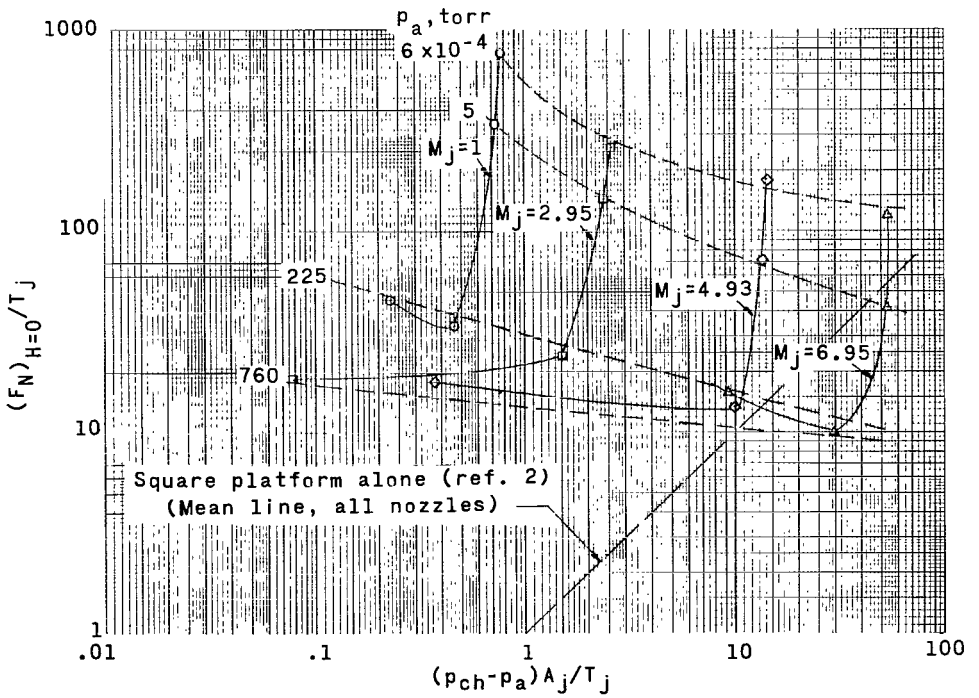

Figure 11.- Variations of the ratio of touchdown normal force to thrust with the maximum force parameter for the square platform.

largest and varied from about 750 for $M_j = 1$ to 120 for $M_j = 6.95$. In comparison, F_N/T_j for the platform without base plate reflections, as obtained from reference 2, was about 1.0 for $M_j = 1$ and about 60 for $M_j = 6.95$. The maximum amount of force ratio amplification in the near-field region due to adding the circular base plate was about 750:1 and 2:1 for the two nozzles of this example. The force ratios at 5 torr (approximate Martian surface pressure) were less but remained large and equal to about 350 for $M_j = 1$. Increasing the ambient pressure further to 225 torr served to reduce the normal load markedly. Between 225 and 760 torr, the variations of maximum force ratio leveled off; and the change in trend may be due largely to the fact that the jet characteristics were changed from underexpanded to overexpanded exit flow. The lowest value of F_N/T_j was about 10 for the Mach number 6.95 nozzle at 760 torr. The results also show that the corresponding reflected loads on the circular base plate (figs. 6 to 9) were only slightly lower than those of the platform. Therefore, it appears that the multireflected streamlines and, possibly, shock waves under near-vacuum conditions for the biplane arrangement were the main cause for the large impingement load amplification. The effects of reflections for the near-field cases are large and significant for structural and control design.

CONCLUSIONS

An investigation was conducted in a vacuum sphere to determine the static, normal impingement loads due to air jets issuing perpendicular from a circular base plate and reflecting off a square platform. The nozzles had nominal exit Mach numbers of 1, 3, 5, and 7. The normal separation distance between the plates varied from about 0 to 100 nozzle exit diameters. The ambient pressures were 6×10^{-4}, 5, 225, and 760 torr. The following observations were made:

1. For both the platform and base plate, the variations of the ratio of normal force to gross thrust with plate separation distance were similar for all the tests in that each had distinguishable near-field, transition, and far-field loads.

2. The near-field force-thrust ratios on both the platform and base were constant for each case at small separation distances and were very large. At an ambient pressure of 6×10^{-4} torr, the force ratio varied from about 750 for the Mach 1 nozzle to 120 for the Mach 7 nozzle. Increasing the exit Mach number or the ambient pressure decreased the impingement loads.

3. The far-field force-thrust ratios also were constant but at much lower values. The force ratios obtained for the platform varied from about 1.3 for a ratio of jet exit pressure to ambient pressure of 10^7 to about 0.8 at a ratio of 10^{-2}.

4. The loads at the transition distances between far-field and near-field conditions varied markedly, combinations of load reversals and rapid changes in magnitude occurring.

5. A comparison of the near-field results for tests with and without base plate reflections indicated that the platform force-thrust ratio was increased by the multiwave reflections about 750:1 for Mach 1 and 2:1 for Mach 7 under near-vacuum ambient pressures and very small separation distances. For the far-field tests, where the plates experienced few, if any reflections, there was little or no amplification of the loads.

Langley Research Center,
National Aeronautics and Space Administration,
Hampton, Va., May 1, 1972.

REFERENCES

1. Goldman, R. L.: Staging Loads. NASA SP-8022, 1969.

2. Hoffman, Sherwood; and Janos, Joseph J.: Forces Due to Air and Helium Jets Impinging Normal to a Flat Plate for Near-Vacuum and Sea-Level Ambient Pressures. NASA TN D-7002, 1971.

3. Gaunter, James W.; Livingood, John N. B.; and Hrycak, Peter: Survey of Literature on Flow Characteristics of a Single Turbulent Jet Impinging on a Flat Plate. NASA TN D-5652, 1970.

4. Janos, Joseph J.; and Hoffman, Sherwood: Force and Moments Produced by Air and Helium Jets Exhausting Parallel to a Flat Plate in a Near Vacuum. NASA TN D-4408, 1968.

5. Janos, Joseph J.; and Hoffman, Sherwood: Forces and Moments Due to Air Jets Exhausting Parallel to Large Flat Plates in a Near Vacuum. NASA TN D-5147, 1969.

6. Ames Research Staff: Equations, Tables, and Charts for Compressible Flow. NACA Rep. 1135, 1953. (Supersedes NACA TN 1428.)

7. Buhler, R. D.; and Nagamatsu, H. T.: Condensation of Air Components in Hypersonic Wind Tunnels – Theoretical Calculations and Comparison With Experiment. GALCIT Mem. No. 13 (Contract No. DA-04-495-Ord-19), Dec. 1, 1952.

8. Kulava, N. M.; and Hosack, G. A.: Supersonic Nozzle Discharge Coefficients at Low Reynolds Numbers. AIAA J., vol. 9, no. 9, Sept. 1971, pp. 1876-1879.

"The aeronautical and space activities of the United States shall be conducted so as to contribute . . . to the expansion of human knowledge of phenomena in the atmosphere and space. The Administration shall provide for the widest practicable and appropriate dissemination of information concerning its activities and the results thereof."

—NATIONAL AERONAUTICS AND SPACE ACT OF 1958

NASA SCIENTIFIC AND TECHNICAL PUBLICATIONS

TECHNICAL REPORTS: Scientific and technical information considered important, complete, and a lasting contribution to existing knowledge.

TECHNICAL NOTES: Information less broad in scope but nevertheless of importance as a contribution to existing knowledge.

TECHNICAL MEMORANDUMS: Information receiving limited distribution because of preliminary data, security classification, or other reasons.

CONTRACTOR REPORTS: Scientific and technical information generated under a NASA contract or grant and considered an important contribution to existing knowledge.

TECHNICAL TRANSLATIONS: Information published in a foreign language considered to merit NASA distribution in English.

SPECIAL PUBLICATIONS: Information derived from or of value to NASA activities. Publications include conference proceedings, monographs, data compilations, handbooks, sourcebooks, and special bibliographies.

TECHNOLOGY UTILIZATION PUBLICATIONS: Information on technology used by NASA that may be of particular interest in commercial and other non-aerospace applications. Publications include Tech Briefs, Technology Utilization Reports and Technology Surveys.

Details on the availability of these publications may be obtained from:

SCIENTIFIC AND TECHNICAL INFORMATION OFFICE

NATIONAL AERONAUTICS AND SPACE ADMINISTRATION

Washington, D.C. 20546